J. Fluid Mech. (1970), *vol.* 44, *part* 1, *pp.* 51–63
Printed in Great Britain

Some cavitation experiments with dilute polymer solutions

By CHRISTOPHER BRENNEN
California Institute of Technology, Pasadena, California

(Received 13 November 1968 and in revised form 23 January 1970)

Experiments on fully developed cavity flows were carried out with the prime initial objective of investigating the effects of the addition of small quantities of 'turbulent drag reducing additive' upon the cavity-surface boundary-layer instability and transition reported in the previous paper (Brennen 1970). However, in most instances, the additives were found to cause an unforeseen instability in the wetted surface flow around the headform. Upon convection, the resulting disturbances dramatically disfigured the cavity surface, thus negating the original purpose. This new phenomenon warranted investigation and became the principal subject of this paper.

1. Introduction

In recent years there has been a growing interest in the turbulent drag reduction in liquid flows achieved by the addition of small quantities of long-chain molecular polymer (and other substances). This has stimulated research on other properties of these dilute solutions such as the effect upon hydrodynamic stability. Earlier investigations (Brennen 1970) concern a flow in which a boundary-layer instability and transition can be observed with virtually no instrumentation. The small vertical water tunnel of figure 1 was adapted to study the influence of additives on fully developed cavities in general and on that instability in particular. As will be seen the latter objective was necessarily abandoned and replaced by a study of an unforeseen instability which the additive caused in the wetted surface flow around the headform.

2. Apparatus

When the ducting and upper tank were filled with liquid, the vertical, gravity-driven tunnel was set in motion by opening the sudden release flap. On completion of the run this flap was closed and the system refilled by a small centrifugal pump. The capacitance wave probe recorded the level of the fluid in the upper tank as a function of time during each run. These records showed that apart from small intervals at the beginning and end, the level fell at a virtually constant rate during a run; they also confirmed the observation that there was little surface disturbance in the upper tank. A theoretical, 'uniform stream velocity' of flow in the working section (U_T) was computed from the slope of the level/time record

and the ratio of cross-sectional areas of the upper tank and working section. Values of U_T in the range 5–40 ft./sec could be obtained by adjustment of the variable orifice or iris.

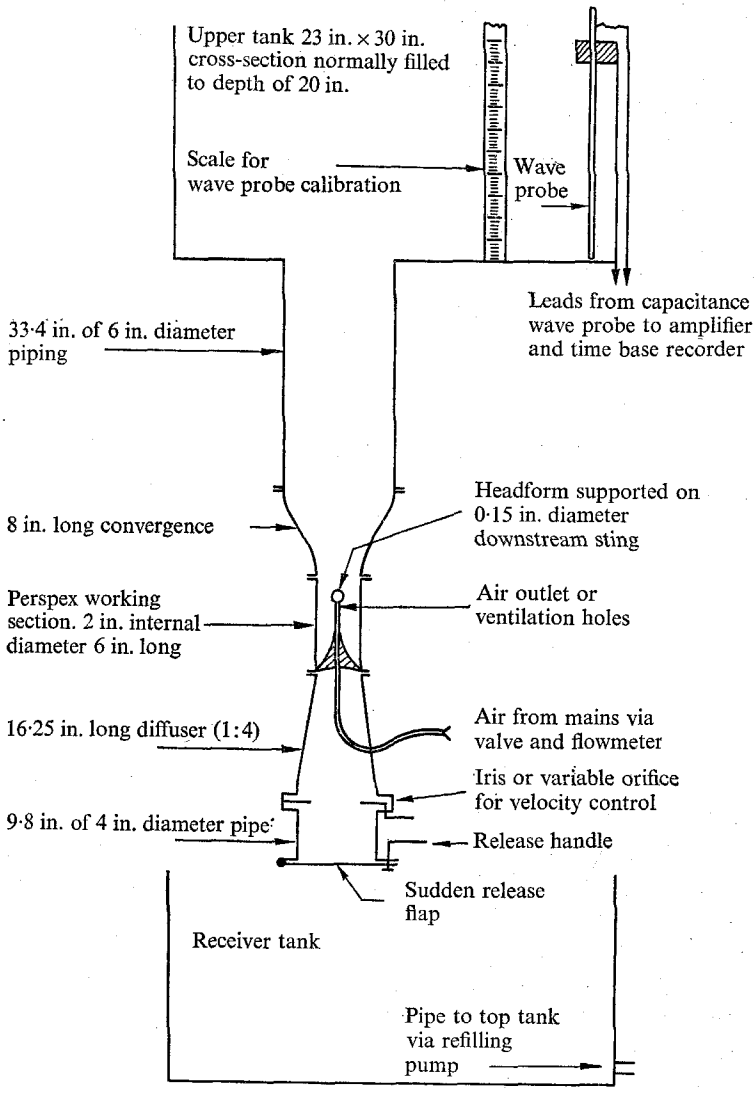

FIGURE 1. The vertical gravity-driven water tunnel.

Four different headforms were supported on the 0·15 in. diameter downstream sting; $\frac{1}{2}$ in. and $\frac{1}{4}$ in. diameter spheres (brass ball bearings), a $\frac{1}{4}$ in. diameter cylinder extending across the width of the working section and a 0·3 in. diameter disk (the last two being set normal to the stream). Cavities behind these headforms could be ventilated, the air travelling from the main via a valve and flowmeter, up the hollow sting and emerging through holes 0·1 in. from the back of the sphere or cylinder or 0·16 in. from the face of the disk.

Although fairly large natural cavities resulted from running at the higher

speeds (25→40 ft./sec) without the introduction of air, ventilation had to be used to produce fully developed cavities at the lower tunnel velocities. Some standardization was achieved by employing, in all of the present experiments, ventilation sufficient to yield choked cavity flow. Thus, for all runs with a particular headform, the cavitation number ($\sigma = (p_u - p_c)/\frac{1}{2}\rho U_T^2$, where p_u, p_c are the 'uniform stream' and cavity pressures, ρ the density of the liquid) could be assumed to be relatively constant and could be estimated as $\delta^2 - 1$, δ being the ratio of the cross-sectional area of the working section to that of the flow at the point of maximum width of the cavity (Birkhoff & Zarantonello 1957). Excessive ventilation for which the jets of air issuing from the holes in the sting appreciably disturbed the cavity surface, had to be avoided.

Still photographs of the cavities were taken in the middle of each run using an electronic flash with a duration of about 30 μsec. But even this flash was not short enough to avoid some blurring of the photographs at the highest flow velocities. The camera shutter operated a pulse on the second channel of the time base recorder thus identifying the precise point in the run at which the photograph had been taken.

A number of high-speed cine films were also made using a Fastax camera. However, even at the maximum film speed (6000 frames/sec) the fluid motions could be satisfactorily discerned only for the lower flow speeds (U_T less than about 20 ft./sec).

3. Additives

Solutions of five different substances were employed in the experiments:

I. A surface-tension-reducing agent, Teepol.

II. Three long-chain molecule polymers: (i) Polyethylene oxide (Union Carbide 'Polyox' WSR 301). (ii) Polyacrylimide (Dow 'Separan' AP 30). (iii) The naturally occurring guar gum.

III. A complex, cationic soap system obtained by correctly mixing an equimolar solution of cetyltrimethylammonium bromide (Cetrimide) and α-naphthol so as to create a micelle structure in the liquid (Nash 1958).

Before each run with these solutions a sample was removed from the upper tank and tested for turbulent drag reduction in a rotating wheel rig previously used by Gadd (1965). Readings from this rig are quoted below as a percentage of the drag in water.

The fresh solutions of Polyox and Separan, made up in the top tank, were measurably degraded after a single run, due, perhaps, to the fairly violent splashing of the liquid in the receiver tank. Wheel rig tests showed that the degradation incurred by the action of the centrifugal pump when refilling the system was small by comparison. Individual solutions liable to degradation were used for about five consecutive runs during which a 50 p.p.m. Polyox solution, for example, would degrade from a value of about 60 % to one around 85 % when tested in the wheel rig.

4. Cavities with water

The cavities produced in water behind the sphere and cylinder headforms exhibited the same wave formation on the cavity surface investigated and analyzed in the earlier paper mentioned above (Brennen 1970). The waves, whose crests ran normal to the direction of mean fluid flow, appeared some distance after separation. At the higher tunnel velocities they grew in amplitude during convection downstream until they broke up yielding a turbulent surface (figure 2(*c*), plate 1). However, below a certain tunnel velocity break up ceased to occur and the waves persisted along the length of the cavity (figure 2(*b*), plate 1). The wave patterns obtained in the present apparatus were somewhat less regular than those obtained in the no. 2 Ship Division, NPL water tunnel probably due, in part, to some non-uniformity in the stream flow. Measured wavelengths lay close to an extrapolation to the origin of the mean line through the experimental results of figures 9 and 10 of that previous paper. However, the present experiments showed that as the velocity or R_{δ_2} (Reynolds number based on momentum thickness of the separated boundary layer—see figure 9, Brennen (1970)) was reduced below a value of about 60 the wave pattern virtually disappeared as in figure 2(*a*), plate 1. Taken in conjunction with the additional effects of surface tension and longitudinal surface curvature, this would be compatible with the absence of any wave patterns on the surface of cavities behind the 3 in. diameter disk of those previous experiments. Predictably then, the 0·3 in. disk of the present experiments produced similarly 'clear' cavities.

The positions of separation, θ, for both spheres and the cylinder have been plotted against a Reynolds number, $R = U_T D/\nu$, based on tunnel velocity and headform diameter in figure 4. Estimated cavitation numbers for the $\frac{1}{4}$ in. sphere, $\frac{1}{2}$ in. sphere and cylinder experiments (see § 2) were 0·1, 0·25 and 0·5 respectively. Previous experiments at a higher range of R had indicated that for a given σ the separation location moved downstream and away from the theoretical, potential flow position (obtained using the smooth separation condition) as R was decreased (Brennen 1969*a*). The present data provide a sensible and monotonic extension of that trend (see Brennen 1969*b*) and the difference between the curves for the $\frac{1}{4}$ in. and $\frac{1}{2}$ in. spheres is typical of the downstream shift caused by a change of σ from 0·1 to 0·25.

In the light of the 'meniscus' appearance of the cavity surface profile at separation, especially pronounced at the lower speeds (e.g. figure 2(*a*)), it seemed likely that variation in surface tension would influence the observed position of separation. Surprisingly, then, the addition of sufficient Teepol to the water to reduce the surface tension from 0·146 lb/ft. to 0·063 lb/ft. had no measurable effect either on θ (see figure 4; first graph) or on any other aspect of the cavity appearance in the photographs. This suggests that the fact that the cavity surface is far from being tangential to the sphere at separation results almost entirely from the presence of the boundary layer rather than from any surface-tension effects.

When considering the results of the following sections it is worth bearing in mind that the water cavities behind the $\frac{1}{2}$ in. sphere, $\frac{1}{4}$ in. sphere and cylinder

remained virtually clear (i.e. as figure 2(*a*)) up to about 8, 16 and 11 ft./sec respectively.

5. Cavities with dilute solutions of polymer

Small quantities of polymer additive had no observable effect upon the cavities behind the 0·3 in. disk; these remained completely clear at all speeds. However, it is immediately apparent from the photographs that the additive had a much more dramatic effect upon the cavities behind the spheres and cylinder than the originally envisaged modification of the wave patterns. Indeed it appears that the additive can cause marked instabilities in the attached flow around these headforms. On convection downstream the disturbances produce irregularities in the separation line and cavity surface.

A representative selection was chosen from the large number of possible experiments; those with polymer solutions are described in this section, those with the cationic soap system in the next section.

Fairly typical of the effect of polymer additive was the performance of the $\frac{1}{2}$ in. sphere in a fresh 50 p.p.m. solution of Polyox:

(*a*) $\frac{1}{2}$ *in. sphere, fresh* 50 *p.p.m. Polyox*

At the lowest tunnel speed ($\sim$ 4 ft./sec) there was little visible effect. However, with slight increase in speed, three-dimensional irregularities appeared on the cavity surface (figure 2(*d*), plate 1). Then above about 7 ft./sec the separation line became gradually distorted into a wavy pattern like that of figure 2(*h*), plate 1 or type II, figure 3, and the most upstream points of separation (referred to as peaks) began to show a downstream shift from the separation location for water under the same conditions (figure 4). Further increase in speed caused the troughs in the separation line to become sharper (type III), finally resulting in the separation appearance of type IV or like that of figure 2(*e*). At the highest tunnel velocities fairly intense spots or trails of turbulence could be detected in the cavity surface 'wake' of each of the separation line troughs (e.g. figure 2(*i*), plate 1).

The pronounced irregularities in the cavity surface appeared to contain a typical longitudinal wavelength, observable in the cavity profile, and a typical spanwise wavelength of the same order of magnitude reflected in the separation line (ϵ). These decreased sharply with increasing speed. The shift in separation compared with that for water, with which is associated a narrowing of the cavities, was somewhat smaller at the highest speeds.

The following were the significant differences in the performance of the other headforms in fresh solutions of 50 p.p.m. Polyox.

(*b*) $\frac{1}{4}$ *in. sphere, fresh* 50 *p.p.m. Polyox*

(i) Both surface and separation irregularities were observed even at the lowest speed. (ii) At intermediate speeds the separation pattern of type IV appeared in the modified form, type IV*a* (like that of figure 2(*f*)); the middle of the upturned

U is seemingly hollowed out to produce a 'pincer' pattern. Since this reverted to the basic type IV when ϵ decreased sufficiently (as in figure 2 (i)) it seems likely that the 'pincer' pattern is an effect of the large ratio of spanwise wavelength to axisymmetric curvature in this case.

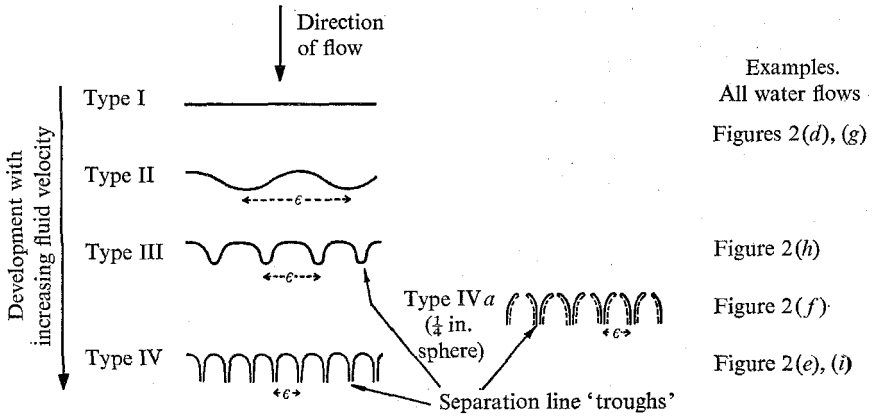

FIGURE 3. Types of separation line distortion occurring with the dilute polymer solutions, indicating the progressive development of that distortion. Wetted surface above the lines, cavity below. The lateral wavelength of the irregularities is ϵ.

(c) $\frac{1}{4}$ *in. cylinder, fresh* 50 *p.p.m. Polyox*

(i) Surface irregularities were observed at all speeds, separation line distortion above about 8 ft./sec. (ii) A major difference was the absence of any significant separation shift (see figure 4).

High-speed films of case (b) showed that the peaks and troughs in the separation line did move around in the lateral direction in what appeared to be a fairly random manner and with a speed smaller than the mean fluid velocity. This seemed to exclude any connexion between the irregularities and particular surface roughnesses.

A number of other experiments were carried out to investigate how the effects were influenced by changes in the Polyox solution.

(d) *Ageing and degradation (as defined in Brennen & Gadd 1967)*

Experiments with the $\frac{1}{4}$ in. sphere in a 50 p.p.m. Polyox solution which had been aged for 8 days (see figure 2 (g), (h) and (i)) and general observation of the effects of degradation indicated that both processes produced: (i) More even patterns of disturbance, presumably due to the increased homogeneity of the solution. (ii) No measurable effect on the magnitude of the spanwise wavelength exhibited at a particular speed (see figure 5). (iii) Slight increase in the critical speeds at which the various types of irregularity and distortion occurred. Compared with figures 2 (g) and (h), for example, fresh Polyox yielded distortion of types III and IV a respectively. But even in the most degraded solution (wheel rig reading of 92 %) these threshold speeds were not raised by more than about 3 ft./sec.

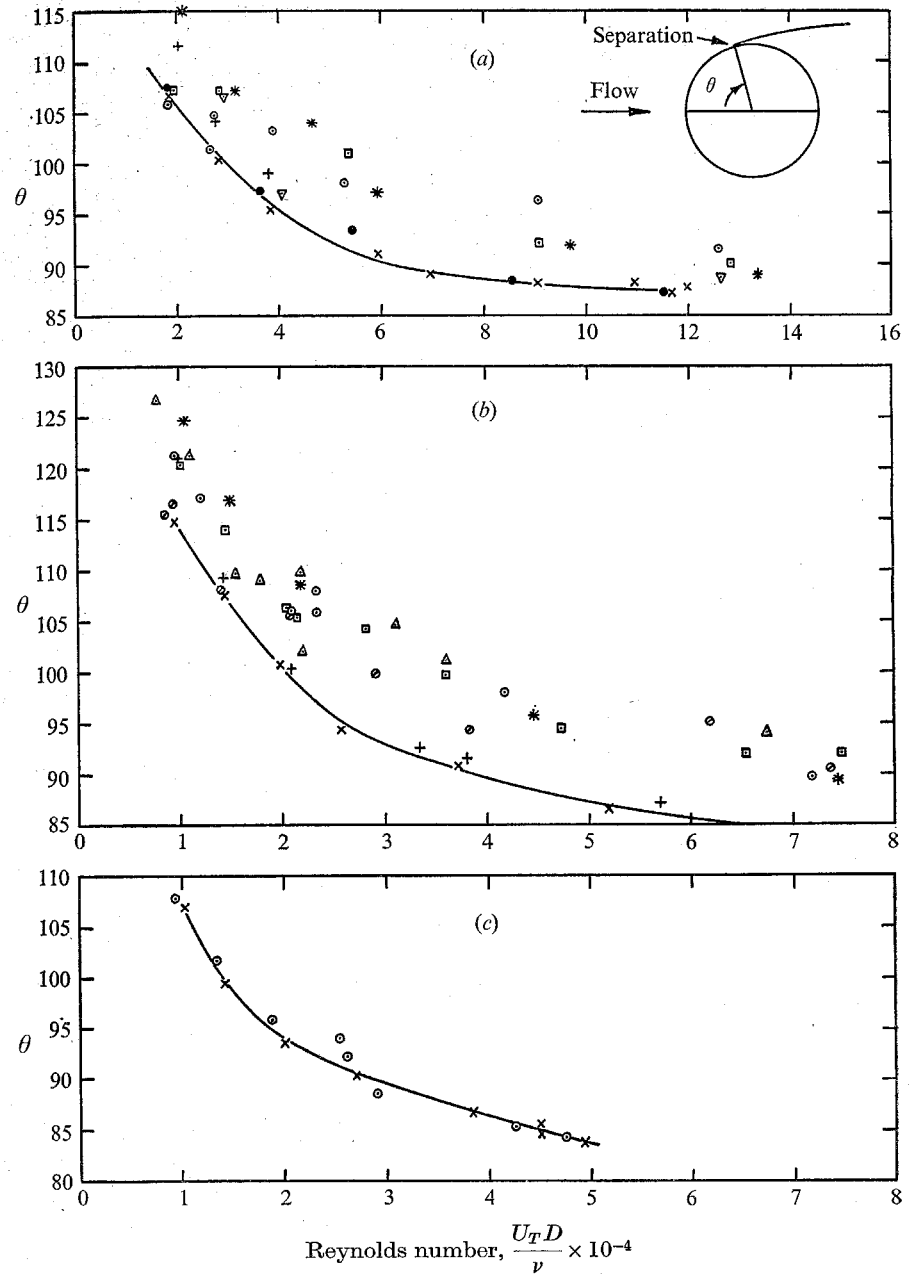

FIGURE 4. Angle of separation, θ, against Reynolds number. ×, water; ○, 50 p.p.m. Polyox; ⌀, 50 p.p.m. aged Polyox; △, 100 p.p.m. Polyox; □, 50 p.p.m. Separan; ▽, 50 p.p.m. guar gum; ●, Teepol; +, 508 p.p.m. Cetrimide/α-naphthol; *, 1524 p.p.m. Cetrimide/α-naphthol. (*a*) $\frac{1}{2}$ in. sphere. (*b*) $\frac{1}{4}$ in. sphere. (*c*) Cylinder.

(*e*) *Concentration*

A number of experiments also indicated that limited changes in concentration had no effect upon ϵ, but may alter the critical speeds: (i) An increase to 100 p.p.m. of Polyox had virtually no effect on the cavities behind the $\frac{1}{4}$ in. sphere. (ii) At 15 ft./sec distortion of separation from the cylinder was of type IV in solutions of 50, 20 and 10 p.p.m. Only with a 5 p.p.m. solution, which incidentally degraded more rapidly than the higher concentrates, did there appear to be any weakening towards types III or II.

Compared with Polyox the effects of the other polymers can be summarized as follows:

(*f*) *Separan*

Solutions of 50 p.p.m. Separan exhibited the same behaviour, with virtually the same ϵ (see figure 5), except that in fresh condition the critical speeds were slightly above those of fresh 50 p.p.m. Polyox.

(*g*) *Guar gum*

On the other hand, 50 p.p.m. of guar gum had a much reduced effect. At all speeds the separation position was very close to that for water (figure 4) with only the odd irregularity in the separation line (figure 2 (*j*) and (*k*), plate 1). However, the cavity surface irregularities were considerably greater than with water and at the lower speeds appeared to contain a predominance of longitudinal disturbance (figure 2 (*j*)) which may account for the lack of separation line distortion. At the higher speeds this gave way to the kind of 'streaky' surface of figure 2 (*k*).

The positions of the upstream limits of the separation lines have been plotted against $U_T D/\nu$ in figure 4, the value used for ν being that for water in all cases since the maximum expected change (4 or 5 %) in viscosity due to the polymer additive (Brennen & Gadd 1967) would have little effect on the resulting graphs. The spanwise wavelengths, ϵ, are presented in figure 5 and appear to be relatively independent of anything but fluid velocity.

Hoyt (1966) photographed natural cavities in water and in 50 p.p.m. Polyox behind an axisymmetric headform (3 in. diameter at separation) at a tunnel speed of 25 ft./sec and observed that the Polyox cavity was much more striated. The average distance between each striation ($\sim$ 0·04 in.) is plotted in figure 5. Hoyt (1967) also reproduced photographs taken by Ellis of a natural cavity on a hemispherical headform ($\frac{1}{4}$ in. diameter) at a speed of about 45 ft./sec. Although the cavity is very thin, resulting in interference from the cylindrical surface, the characteristic type IV separation can be detected and the value of ϵ (figure 5) agrees with the present experiments.

6. Cavities with solutions of Cetrimide α-naphthol

The $\frac{1}{2}$ and $\frac{1}{4}$ in. spheres were tested in solutions of 508 and 1524 total p.p.m. of the cetrimide/α-naphthol soap system. In the rotating wheel rig both concen-

trations yielded turbulent drag reduction of the same order as fresh 50 p.p.m. Polyox. They also exhibit strong viscoelasticity, at least at low shear rates; when swirled in a beaker, for example, the swirl decays much more rapidly than with water and there is a visible recoil (Nash 1958).

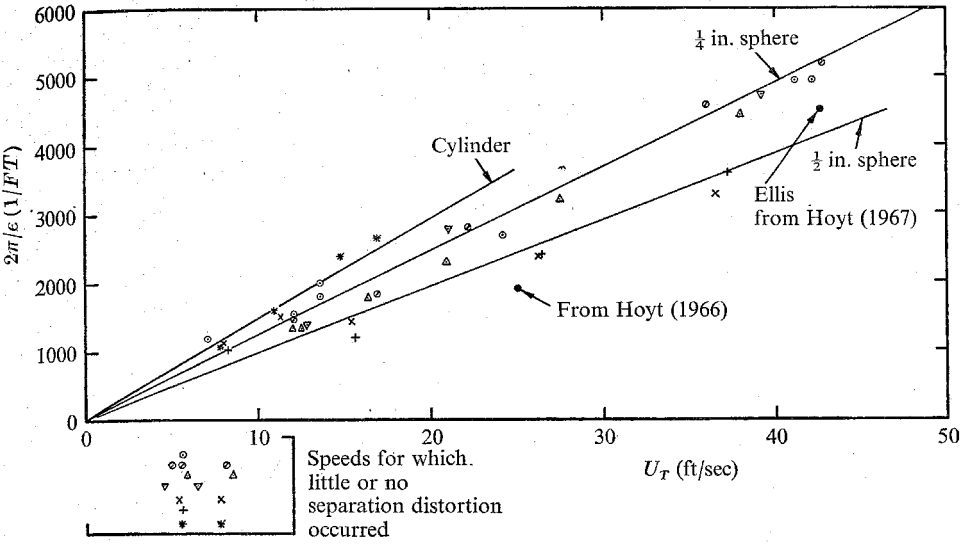

FIGURE 5. Variation of separation distortion wavelength, ϵ, with tunnel velocity, U_T. ¼ in. sphere: ○, 50 p.p.m. Polyox; Ø, 50 p.p.m. aged Polyox; △, 50 p.p.m. Separan; ▽, 100 p.p.m. Polyox. ½ in. sphere: ×, 50 p.p.m. Polyox; +, 50 p.p.m. Separan. Cylinder: *, 50 p.p.m. Polyox.

(*a*) ½ *in. sphere*

At all speeds both concentrates produced cavities with three-dimensional surface disturbances similar to those found with Polyox but only slight irregularities in the separation line (e.g. (figure 2(*l*), plate 1)). The surface disturbances were less violent with the 508 p.p.m. solution, especially at the higher speeds. They also seemed more violent immediately after separation than further downstream, suggesting a viscoelastic damping effect during convection along the cavity (figure 2(*l*), plate 1). With the 508 p.p.m. solution there was no downstream shift of separation except at the lowest speed (about 5° at 4 ft./sec), whereas the 1524 p.p.m. solution had a shift of about 8° at all speeds (figure 4).

(*b*) ¼ *in. sphere*

The principal deviation from the performance with the larger headform was that the surface irregularities were more subdued at the lower speeds (figure 2(*m*), plate 2) and gradually disappeared with increasing U_T. Despite this the pattern of separation shift was virtually identical (figure 4).

7. Some conclusions and discussion

With the two spherical headforms, the downstream shift in separation caused by the polymer additive seems to be roughly related to the degree of distortion in the separation line. Though it appears from figure 4 that this is not the case with the cylinder, it is to be noted that only the position of the separation line peaks has been plotted and that there will still be some 'average' downstream shift. The virtually constant 8° shift in the 1524 p.p.m. Cetrimide/α-naphthol solution may have a somewhat different origin since it occurs in the absence of significant separation distortion. White (1967) reported that although a 508 p.p.m. solution was Newtonian, 1000 p.p.m. exhibited pseudoplasticity and a reduction of the non-Newtonian index, n, from 1·0 to 0·9 (at least for low shear rates). Bizzell & Slattery (1962) calculated that such a reduction would cause a downstream shift of 4·6° (8·6° for $n = 0{\cdot}8$) in the separation position for non-cavitating flow around a sphere. The present results would indicate a similar shift in the cavitating case.

Many of the results of both §§ 5 and 6 would suggest that there is some relationship between the strength of the disturbances produced by a particular solution and its turbulent drag-reducing effectiveness. In order to develop some tentative explanation of this it is useful to take note of the following:

(i) In his resistance measurements of pipe flows, White (1968) found that whereas a certain critical wall shear stress, $(\tau_w)_{\text{crit}}$, had to be exceeded before polymer solutions exhibit drag reduction, the Cetrimide/α-naphthol solutions were effective only *up to* a particular τ_w above which, he suggests, the micelle structure may become disrupted. Rough, order of magnitude, estimates of these critical τ_w, taken from White and others, might be: 0·02, 0·09, 0·04 and 0·25 lb/ft.^{2} for fresh Polyox, 6-day-old Polyox, Separan and guar gum: 0·15 and 0·3 lb/ft.^{2} for 508 and 1524 p.p.m. Cetrimide/α-naphthol solution.

(ii) In the nominally laminar wetted surface boundary layer of the present experiments τ_w will presumably increase from zero at stagnation to a maximum value and then fall away again to zero at separation. In the case of a sphere, rough calculations suggest that the peak occurs around $\theta = 60°$ and takes a value of the order of magnitude of $\rho U_T^2/R^{\frac{1}{2}}$: thus typical values of $(\tau_w)_{\max}$ would be as follows:

U_T	5	10	15	20	30	ft./sec
$(\tau_w)_{\max}$ $\frac{1}{4}$ in. sphere	0·5	1·5	2·7	4·2	7·7	lb/ft.^{2}
$(\tau_w)_{\max}$ $\frac{1}{2}$ in. sphere	0·4	1·0	1·9	2·9	5·4	lb/ft.^{2}

(iii) Considerable experimental evidence, summarized in Brennen (1969*b*), indicates that the pressure distribution on the wetted surface of a fully-cavitating sphere (or cylinder) reaches its minimum close to the theoretical, 'smooth separation' position (about 60°) and that between this and the actual separation position the pressure is roughly constant, perhaps rising somewhat. In the case of the disk however, both separation and probably the minimum pressure occur at the sharp edge.

The information for a sphere or cylinder is presented diagrammatically in figure 6 and suggests the following speculative explanation which is consistent with the observations. The region AC is one of strong streamwise acceleration and the flow there is likely to be highly stable: instabilities could, however, arise in the region CD where the flow may even be decelerating. Suppose that during the

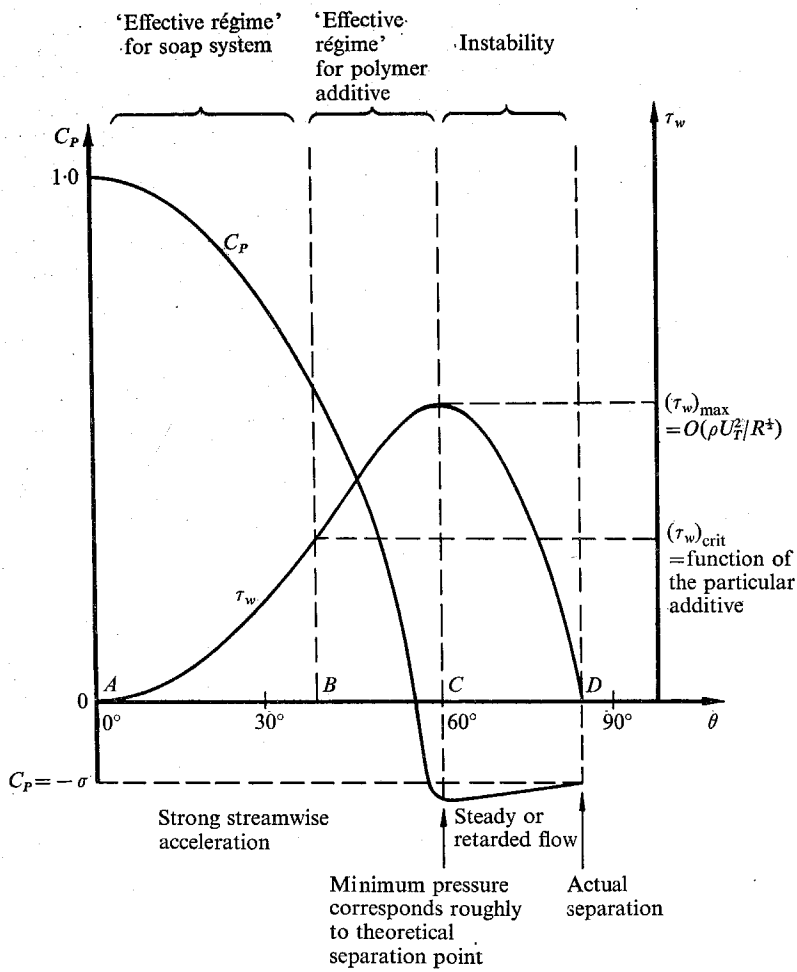

FIGURE 6. Diagrammatic representation of the wetted surface conditions with the sphere and cylinder headforms.

flow through AC elastic energy is stored in the polymer molecules or micelle structure *only* when τ_w is in the effective régime for that particular additive, that is to say BC for a polymer or AB for the soap system. Then after the acceleration ceases the release of this energy in the region CD may lead to the rapid growth of the unstable disturbances which, upon convection, cause the observed separation distortion and cavity surface irregularity. This would be consistent with virtually all the experimental results. For example: (i) The extent of AB decreases whilst BC increases with U_T. This would account for the disturbances in the polymer

solutions becoming progressively more developed whereas those in the Cetrimide/α-naphthol die away with increasing speed. (ii) With the $\frac{1}{4}$ in. sphere $(\tau_w)_{\max}$ is larger than with the $\frac{1}{2}$ in. sphere at a given U_T. Indeed the disturbances in the polymer are greater with the $\frac{1}{4}$ in. sphere, whereas those in the Cetrimide are more pronounced with the $\frac{1}{2}$ in. sphere. (iii) All the $(\tau_w)_{\text{crit}}$ variations with different polymers, aging, degradation and changing concentration fit satisfactorily into this picture. For instance since guar gum has a considerably higher $(\tau_w)_{\text{crit}}$ than Polyox or Separan it is to be expected that it would have a much reduced effect. (iv) The lack of any observable effects with the disk headform is probably due to the absence of a region CD in that case. The different acceleration distribution on the head form surface may, however, also have an effect. (v) The spanwise wavelength of the separation line distortion, ϵ, appears to change little with the size of the headform (figure 5). Indeed it varied significantly only with U_T. This is compatible with the origin of the disturbances being relatively close to the separation line. If, for example, they originated at or upstream of stagnation then it would be expected that ϵ would be twice as large for the $\frac{1}{2}$ in. sphere as for the $\frac{1}{4}$ in. sphere.

There remains the question of the nature of the instability in CD. The regular spanwise distribution might suggest Taylor vortices which could occur in the retarded flow of that region. The experiments of Rubin & Elata (1966), indicating that the Taylor instability is delayed in polymer solutions, should not eliminate this possibility since, if the above conjecture is correct, one of the important features is the particular strain rate history to which the polymer molecules are subjected. Another possibility is the hairpin vortices which develop during transition as described by Stuart (1965). Indeed Pfenniger (1967) suggested that polymer molecules may have an important effect upon these vortices (see also Gadd 1968).

Much of this, however, is speculative and a complete explanation must await a detailed exploration of the exact nature of the disturbances, their formation and growth. It does not seem unreasonable, however, to suggest that these instabilities may also occur in comparable fully-attached flows, such as those of Sanders (1967). If this is the case the cavities may have been used as a very rough 'flow visualization' device.

The experiments were carried out as part of the research programme of the Ship Division of the National Physical Laboratory. The author is deeply indebted to David Swindells, who took responsibility for the photography and produced such excellent results. I also wish to thank Dr G. E. Gadd for valuable discussions on the subject-matter.

REFERENCES

Birkhoff, G. & Zarantonello, E. H. 1957 *Jets, Wakes and Cavities*. New York: Academic.

Bizzell, G. D. & Slattery, J. C. 1962 Non-newtonian boundary layer flow. *Chem. Engng Sci.* **17**, 713.

Brennen, C. & Gadd, G. E. 1967 Ageing and degradation in dilute polymer solutions. *Nature, Lond.* **215**, 1368.

BRENNEN, C. 1969*a* A numerical solution of axisymmetric cavity flows. *J. Fluid Mech.* **37**, 671.

BRENNEN, C. 1969*b* Some viscous and other real fluid effects in fully developed cavity flows. *Cavitation State of Knowledge.* New York: ASME.

BRENNEN, C. 1970 Cavity surface wave patterns and general appearance. *J. Fluid Mech.* **44**, 33.

GADD, G. E. 1965 Turbulence damping and drag reduction produced by certain additives in water. *Nature, Lond.* **206**, 463.

GADD, G. E. 1968 Effects of drag-reducing additives on vortex stretching. *Nature, Lond.* **217**, 1040.

HOYT, J. W. 1966 Effect of high-polymer solutions on a cavitating body. *Proc. 11th International Towing Tank Conference, Tokyo.*

HOYT, J. W. 1967 The influence of polymer-secreting organisms on fluid friction and cavitation. *U.S. Naval Ordnance Test Station Report,* NOTS TP 4364.

NASH, T. 1958 The interaction of some naphthalene derivatives with a cationic soap below the critical micelle concentration. *J. Colloid. Sci.* **13**, 2.

PFENNINGER, W. 1967 A hypothesis of the reduction of the turbulent friction drag in fluid flows by means of additives, etc. *4th Winter Meeting of the Society of Rheology.*

RUBIN, H. & ELATA, C. 1966 Stability of Couette flow of dilute polymer solutions. *Phys. Fluids*, **9**, 10.

SANDERS, J. V. 1967 Drag coefficients of spheres in poly(ethylene oxide) solutions. *Int. Ship. Prog.* **14**, 153.

STUART, J. T. 1965 The production of intense shear layers by vortex stretching and convection. *N.P.L. Aero. Rep.*, 1147.

WHITE, A. 1967 Drag of spheres in dilute high polymer solutions. *Nature, Lond.* **216**, 995.

WHITE, A. 1968 Studies of the flow characteristics of dilute high polymer solutions. *Bull.* no. 5. *Hendon College of Technology, Research.*

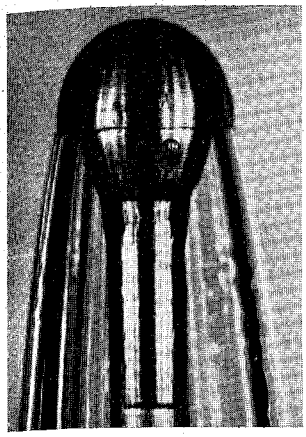

(*a*)

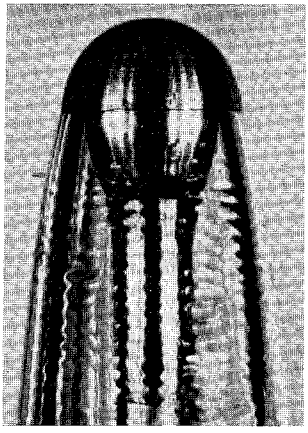

(*b*)

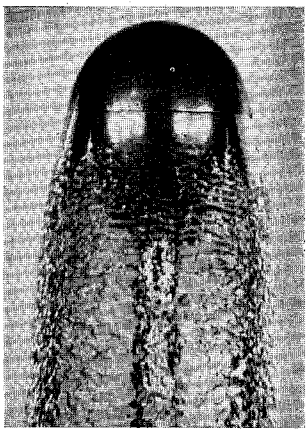

(*c*)

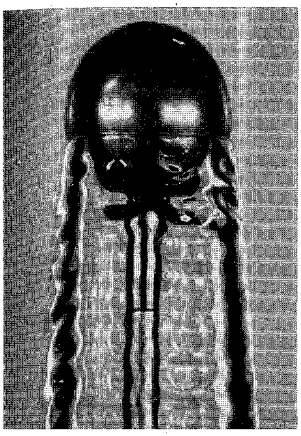

(*d*)

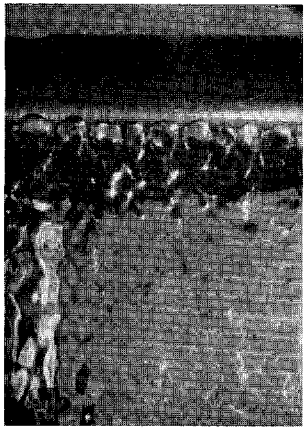

(*e*)

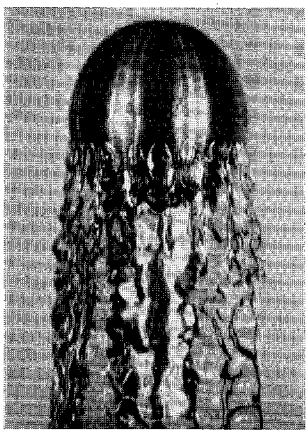

(*f*)

(*g*)

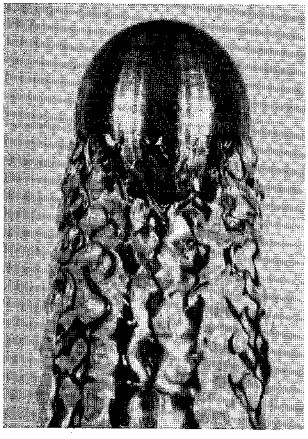

(*h*)

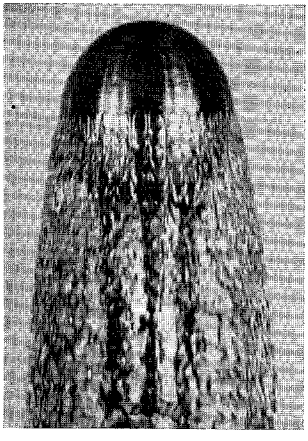

(*i*)

FIGURE 2. For legend see overleaf.

(*Facing p.* 64)

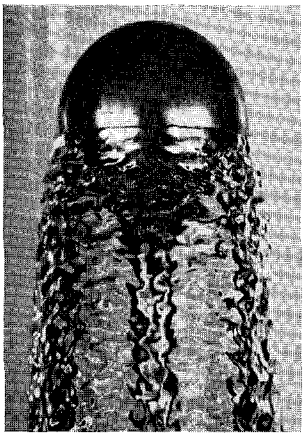

(*j*)

(*k*)

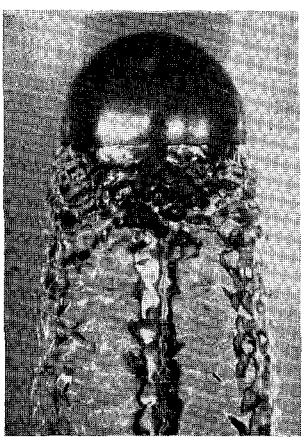

(*l*)

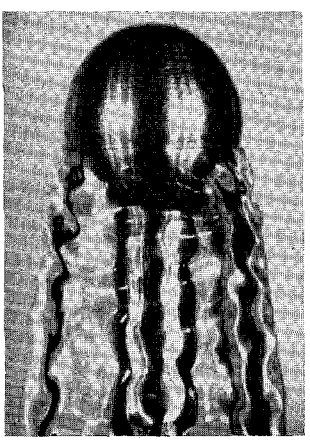

(*m*)

FIGURE 2. High-speed photographs of cavities behind various headforms, in different solutions and at various tunnel velocities, U_T, as shown. Water: (*a*) $\frac{1}{4}$ in. sphere, 11·5 ft./sec; (*b*) $\frac{1}{4}$ in. sphere, 21·6 ft./sec; (*c*) $\frac{1}{2}$ in. sphere, 26·3 ft./sec. Fresh 50 p.p.m. Polyox: (*d*) $\frac{1}{2}$ in. sphere, 5·4 ft./sec; (*e*) cylinder, 10·9 ft./sec; (*f*) $\frac{1}{4}$ in. sphere, 13·6 ft./sec. Aged 50 p.p.m. Polyox: (*g*) $\frac{1}{4}$ in. sphere, 8·2 ft./sec; (*h*) $\frac{1}{4}$ in. sphere, 12·1 ft./sec; (*i*) $\frac{1}{4}$ in. sphere, 36·0 ft./sec. 50 p.p.m. guar gum: (*f*) $\frac{1}{2}$ in. sphere, 11·8 ft./sec; (*k*) $\frac{1}{2}$ in. sphere, 36·7 ft./sec. Cetrimide/α-naphthol: (*l*) 1524 p.p.m., $\frac{1}{2}$ in. sphere, 13·5 ft./sec; (*m*) 508 p.p.m.; $\frac{1}{4}$ in. sphere, 8·3 ft./sec.